2012 22nd International Lightning Detection Conference
2 – 3 April • Broomfield, Colorado, USA
4th International Lightning Meteorology Conference
4 – 5 April • Broomfield, Colorado, USA

LIGHTNING DISTRIBUTION AND EYEWALL OUTBREAKS IN TROPICAL CYCLONES DURING LANDFALL

Wenjuan Zhang*[1], Yijun Zhang[1,2], Dong Zheng[1], Xiuji Zhou[1,2]
[1]Laboratory of Lightning Physics and Protection Engineering, Chinese Academy of Meteorological Sciences, Beijing, China
[2]State Key Laboratory of Severe Weather, Chinese Academy of Meteorological Sciences, Beijing, China

1. INTRODUCTION

With the development of lightning detecting technologies in the last two decades, observations have determined that lighting in tropical cyclones may be a more common event than originally thought and studies began to investigate frequency and distribution of lightning in tropical cyclones. Land-based lightning detection networks allow monitoring lightning in TCs within a few hundred kilometers of the coast. Samsury and Orville (1994), using the National Lightning Detection Network (NLDN) data, described the distribution of lightning in Hurricanes Hugo and Jerry (1989) as they made landfall, and found the majority of flashes located in the right front and right rear quadrants. Molinari et al. (1994, 1999), also with the NLDN data, found a common radial distribution of lightning in nine North Atlantic basin hurricanes. Lyons and Keen (1994) examined lightning in four tropical storms in the Gulf of Mexico using Lightning Position and Tracking System (LPATS) data, and found lightning was common within the outer rainbands while absence within the interior of mature TCs. More recently, Fierro et al. (2011) provided a first insight into the three-dimensional electrical activity with the Los Alamos Sferics Array (LASA) and investigated the inner core lightning with changes of storm intensity in Hurricanes Katrina and Rita (2005). Abarca et al. (2011) studied 24 Atlantic basin TCs with the World Wide Lightning Location Network (WWLLN) data and suggested flash density in the inner core was potential for distinguishing intensifying versus non-intensifying TCs.

The predictive values of cloud-to-ground (CG) lightning to structure and intensity changes of TCs have been discussed recently. Squires and Businger (2008) analyzed the morphology of eyewall lightning in two category 5 hurricanes and found each hurricane produced eyewall outbreaks during the period of rapid intensification (RI), replacement cycles (RC), and the period encompassed the maximum intensity (MI). Molinari et al. (1999) proposed the indications of eyewall lightning outbreaks in the following: an outbreak in a weakening, steady or slowly deepening hurricane might indicate a rapidly intensification; an outbreak in a hurricane deepening for some time may indicate the imminent end or reversal of intensification; the lack of inner core flashes may indicate little change in the hurricane. Price et al. (2009) observed a statistical

* *Corresponding author address:* Wenjuan Zhang, Laboratory of Lightning Physics and Protection Engineering, Chinese Academy of Meteorological Sciences, Beijing, China, 100081. E-mail: zhangwj@cams.cma.gov.cn.

increase of lightning activity approximately one day before the peak winds. Fierro et al. (2011) revealed an increase in discharge heights during RI and suggested that the IC narrow bipolar events (NBEs) were useful in tracking the evolution of strong convection during intensification. Furthermore, increasing CG flash rates could also accompany or precede a weakening of weak TCs and/or an imminent change in its track (Willoughby 1990; Fierro et al. 2007).

In this work, we use lightning data from a regional lightning detection network in south China, along with storm track and intensity data from China Meteorological Administration (CMA), to study the characteristics of lightning activity during the periods of landfall.

2. DATA AND METHODS

Lightning activities of 33 tropical cyclones (Fig. 1) which made landfall in Guangdong province, south China, from 1999 to 2010, were analyzed. The lightning data were from the Lightning Detection Network of Guangdong Power Grid. The network consists of 16 sensors and provides real-time CG lightning locations for the whole area of Guangdong province and its vicinity covers by the combined technique of magnetic direction finding (DF) and time of arrival (TOA).For the purpose of minimizing variation of location error and detection efficiency with distance, range was limited to 400 km away from the TC center to at least one sensor. By inspecting lightning activities in the eyewall region, defined as within 60 km of the storm center, an eyewall lightning outbreak was determined as: (1) a 50% increase in flash rate (fl/h) from one hour to the next; and (2) the absolute increased count of flash in one hour was larger than the mean flash rate during the time of study.

The information on TC track and intensity were obtained from the *Yearbook of Tropical Cyclone* (CMA 1999-2010) published by the China Meteorological Administration for 1999-2010. It gives the 6-hourly intervals data of center latitude, longitude, maximum sustained surface wind speed and minimum central pressures. Hourly center position and intensity were obtained by Spline Interpolation. TC intensities are classified into six levels depending on the mean maximum wind speed during the lifetime: tropical depression (TD, 10.8-17.1 m s^{-1}), tropical storm (TS, 17.2-24.4 m s^{-1}), severe tropical storm (STS, 24.5-32.6 m s^{-1}), typhoon (TY, 32.7-41.4 m s^{-1}), severe typhoon (STY, 41.5-50.9 m s^{-1}) and super typhoon (Super TY, >51.0 m s^{-1}).

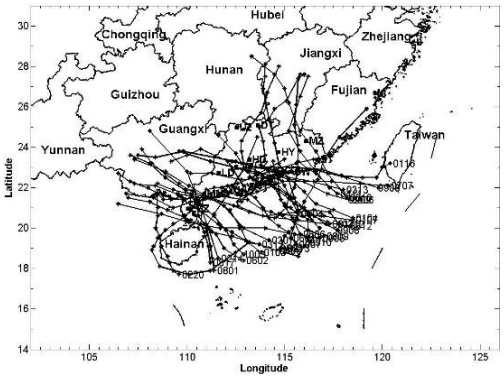

FIG. 1. Center positions for the periods of within 400 km of at least one locating sensor of the 33 tropical cyclones examined in this study.

3. RESULTS

a. Lightning distribution in tropical cyclones at different intensity levels

Figure 2 shows the radial distributions of flash density for TCs of four intensity levels. Tropical storm had a distribution of single peak feature with a maximum flash density in the eyewall region (within 60 km of the center), and the flash density decreased rapidly outside the

eyewall. Severe tropical storm had more intense lightning activities in outer rainband than that in tropical storm and showed a bimodal distribution of flash density in radius. One peak was in the eyewall region similar to tropical storm and the other was located in outer rainband (180-500 km of the center). The radial distributions of lightning in typhoons showed three features: a weak maximum in the eyewall region, a minimum in inner rainband (60-180 km of the center) and a strong maximum in outer rainband. Lightning in severe typhoons had a radial distribution of single peak feature and the maximum flash density was located in outer rainband. Flash densities in the eyewall of severe typhoon and typhoon were much lower than in severe tropical storm and tropical storm. This result was consistent with the study of Atlantic basin hurricanes by Molinari et al. (1999), who found the ground flash density maximum in the core was larger in marginal (32-35 m s^{-1} mean maximum sustained surface wind speed) than in strong (56 m s^{-1}) hurricanes. Although flash densities in the eyewall and outer rainband enormously varied with storm intensity level, low flash density in inner rainband occurred in all the four TC levels (Fig. 2). Table 1 presents the ratios of flash densities between the eyewall and outer rainband for four TC levels. The majority of lightning occurred in the core region for tropical storms, thus storms in this level had the largest ratio (1:0.2) among all the four levels. Although the maximum of flash density was also located at the eyewall in severe tropical storms, lightning in the outer rainband became intense and the ratio of flash densities between the eyewall and outer rainband decreased to 1:0.6. Storms at typhoon level showed a three-zone pattern of lightning, a large eyewall lightning, very little lightning in the inner rainband, and a tremendous amount of lightning in the outer rainbands, and the ratio of flash densities between the eyewall and outer rainband was 1:2.1. When the storm strengthened to severe typhoon intensity, the vast majority of lightning occurred in the outer region and the ratio of flash densities between the eyewall and outer rainband reached the lowest (1:3.9).

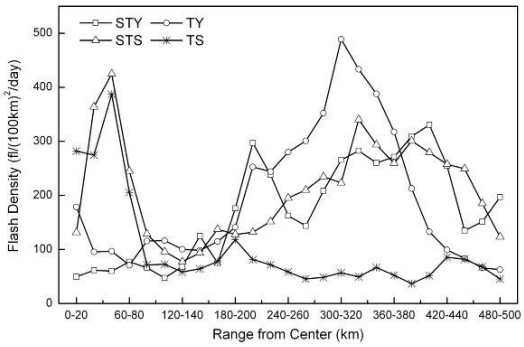

FIG. 2. Radial distribution of CG flash density in four TC intensity levels, computed by averaging storms with the same intensity level.

b. Lightning activity during the period of pre- and post-landfall

Figure 3 presents the radial distribution of flash density during the period of pre- and post-landfall for four intensity categories. Lightning activity was weak in tropical storms when the storms were over water. During the period of post-landfall, the flash rate in the eyewall region increased rapidly but slightly reduced in outer rainband. Severe tropical storm showed a larger lightning frequency then tropical storm during pre-landfall, but the frequency decreased in post-landfall, dramatically in the eyewall region. Outer rainband contained the vast majority of ground flashes in typhoons and severe typhoons before landfall. When the storm was on land, flash density in outer rainband decreased rapidly in severe

typhoons but kept unchanged in typhoons. Flash density in the eyewall region in typhoons appeared a weak maximum after landfall. The results were the averaging values of all the TCs in the same intensity category. It is possible that the distributions are not fit for the characteristic of every storm, but they give an overall picture of lightning activity in storms at different intensity level before and after landfall.

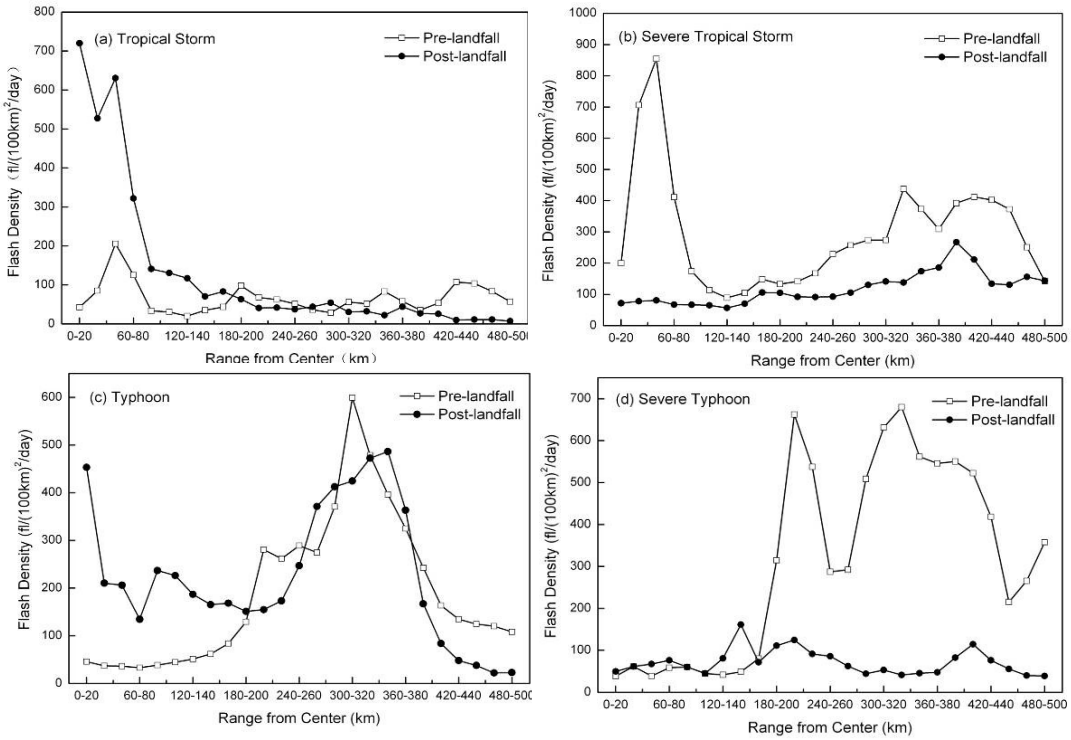

FIG. 3. Radial distribution of flash density during the period of pre- and post-landfall, computed by averaging storms of same intensity category. (a) Tropical storm, (b) Severe tropical storm, (c) Typhoon, (d) Severe typhoon.

TABLE 1. The ratio of flash density between the eyewall and outer rainband in four TC intensity levels, computed by averaging storms with the same intensity. The eyewall region was within 60 km of the storm center and outer rainband was 180-500 km from the center as described in section 2.

Intensity Level	Tropical Storm	Severe Tropical Storm	Typhoon	Severe Typhoon
Ratio	1:0.2	1:0.6	1:2.1	1:3.9

c. Eyewall lightning outbreaks

By using the method described in section 2, totally 62 eyewall flash outbreaks were identified in the sample. Table 2 shows the statistical results of flash outbreaks occurred in the eyewall region. Eyewall lightning bursts occurred mainly in the following four time periods.

1) During the intensification period over water. Nine outbreaks occurred during the period of rapid deepening before the storm landfall. The peak value of maximum sustained wind was preceded by the eyewall flash outbreaks approximately 7.1

h. The storm made landfall averagely 18.6 h after the eyewall outbreaks (Table 2).

2) During the weakening stages of storm intensity. Twenty-seven outbreaks occurred during the periods of intensity weaken, seven in pre-landfall and twenty in post-landfall, which accounted for 43% of the total number of outbreak. With a ratio of positive to total CG flashes of 17.1%, positive lightning was more active during storm weakening periods compared to other periods (Table 2). Thomas et al. (2010), with analysis of North Atlantic hurricanes, also indicated an increase in the relative number of positive CG lightning in the inner core prior to and during periods of storm weakening, and suggested a potential value of eyewall lightning for hurricane intensity change forecasting.

3) During the periods of maximum intensity. Nine outbreaks occurred during the times that encompassed the MI and accounted for 15% of total bursts. The average ratio of positive to total CG flashes during MI period was 10.3%. The time when storm reached MI was averagely 7.8 h ahead of landfall (Table 2).

4) During the periods of recurvature. Eyewall outbreaks were also observed during a steady period of storm with no changes of winds and pressure. The outbreaks were associated with turnings of the storm track. Ten outbreaks in six storms (ie. Typhoon Sam (9908); Typhoon Nari (0116); Severe Tropical Storm Pabuk (0707); Severe Typhoon Fengshen (0806); Tropical Storm Higos (0817); and Severe Tropical Storm Goni (0907)) occurred during this period, and accounted for 11% of all outbreaks.

TABLE 2. Statistical results of eyewall flash outbreaks in all the storms.

Stage	Outbreaks		+CG%		With Landfall	Number of	Hours to landfall	
	Number	%	Mean	Min–Max		Outbreak	Mean	Min–Max
Strengthen	9	15	13.9	3.0–51.9	Pre-landfall	9	18. 6	7–58
Weaken	27	43	17.1	1.8–81.3	Pre-landfall	7	16.9	1–48
					Post-landfall	20	7.9	0–35
MI	9	15	10.3	3.2–17.7	Pre-landfall	9	7.8	2–17
Recurvature	10	16	12.8	1.1–20.5	Pre-landfall	7	25.6	5–36
					Post-landfall	3	15.3	7–25
Uncertain	7	11	8.0	1.9–21.0	Pre-landfall	7	19.4	3–44
Total	62	100				62		

Figure 4 shows an example of eyewall lightning outbreaks during the above three conditions. The figure displays the time variation of eyewall lightning, superimposed on hourly interpolations of the maximum sustained wind speed for Severe Tropical Storm York (9910). York produced a total of five eyewall flash outbreaks during the period of study. The first two occurred during the rapid intensification which began at 0000 UTC 14 September and ended at 0200 UTC 15 September. The maximum sustained surface winds increased from 20 m s^{-1} to

30 m s^{-1} over the 29-h period of intensification, and then kept the peak wind of 30 m s^{-1} for 26 h (i.e. MI stage). During the time York reached MI, a third eyewall outbreak occurred, but much smaller than the first two in flash rates. York made its landfall in Guangdong at 1000UTC 16 September at the wind speed of 27 m s^{-1}. Since then the winds dropped rapidly from 27 m s^{-1} to 12 m s^{-1} in 20 h and the central pressure increased from 977 to 1000. Two eyewall outbreaks occurred during this weakening stage after the storm making landfall.

Figure 5a and 5b show the temporal evolution of eyewall outbreaks and the storm track of Typhoon Nari (0116), respectively. Nari experienced totally six eyewall flash outbreaks during the period of study. The first two outbreaks (Burst ① and ②) occurred during a steady period for the winds kept at 18 m s^{-1} and the pressure kept at ~998 hPa for 36 h (Fig. 5a). Actually these two outbreaks were associated with the storm recurvature which began at 0000 UTC 18 September and ended at 1200 UTC 19 September 2001 (Fig. 5b). Nari made its largest turning angle during the period of study at 0000 UTC 19 September, with the moving direction changed from southwest to west. A great increase of flash rate presented at 2300 UTC 18 September, one hour ahead of the sharp turning. From Figure 8a and 8b it was shown that the eyewall lightning became intense at the beginning of recurvature and increased to a flash peak one hour ahead of the biggest turning point. Nari intensified from TS to STS from 1200 UTC 19 September to 0000 UTC 20 September subsequently and the third and fourth outbreaks (Burst ③ and ④) occurred prior to and during this intensification. The storm intensity decreased rapidly from STS to TS and then to TD after Nari made landfall at 0200 UTC 20 September. The fifth and sixth eyewall outbreaks (Burst ⑤ and ⑥) were associated with this weakening stage.

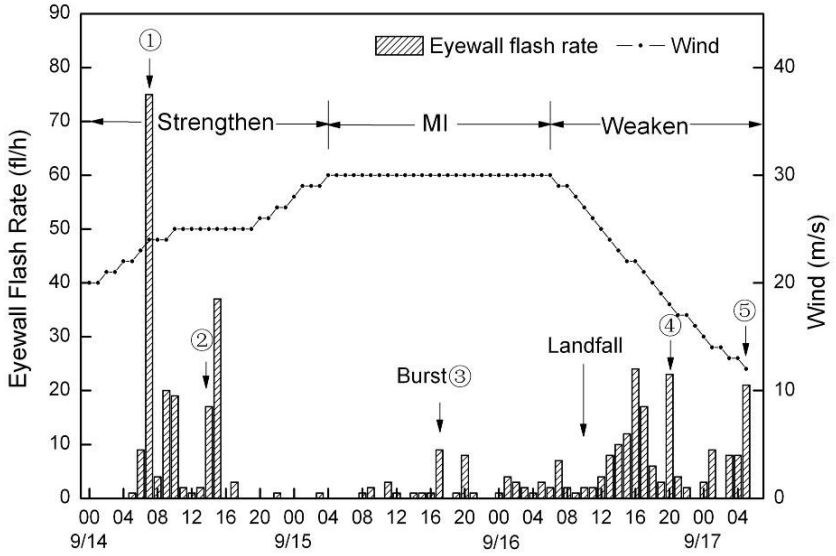

FIG. 4. Temporal evolution of lightning within 60 km of the center of Severe Tropical Storm York (9910) (bars), superimposed on hourly interpolations of the maximum sustained wind speed (line with circles). Eyewall lightning outbreaks are indicated by arrows with serial numbers.

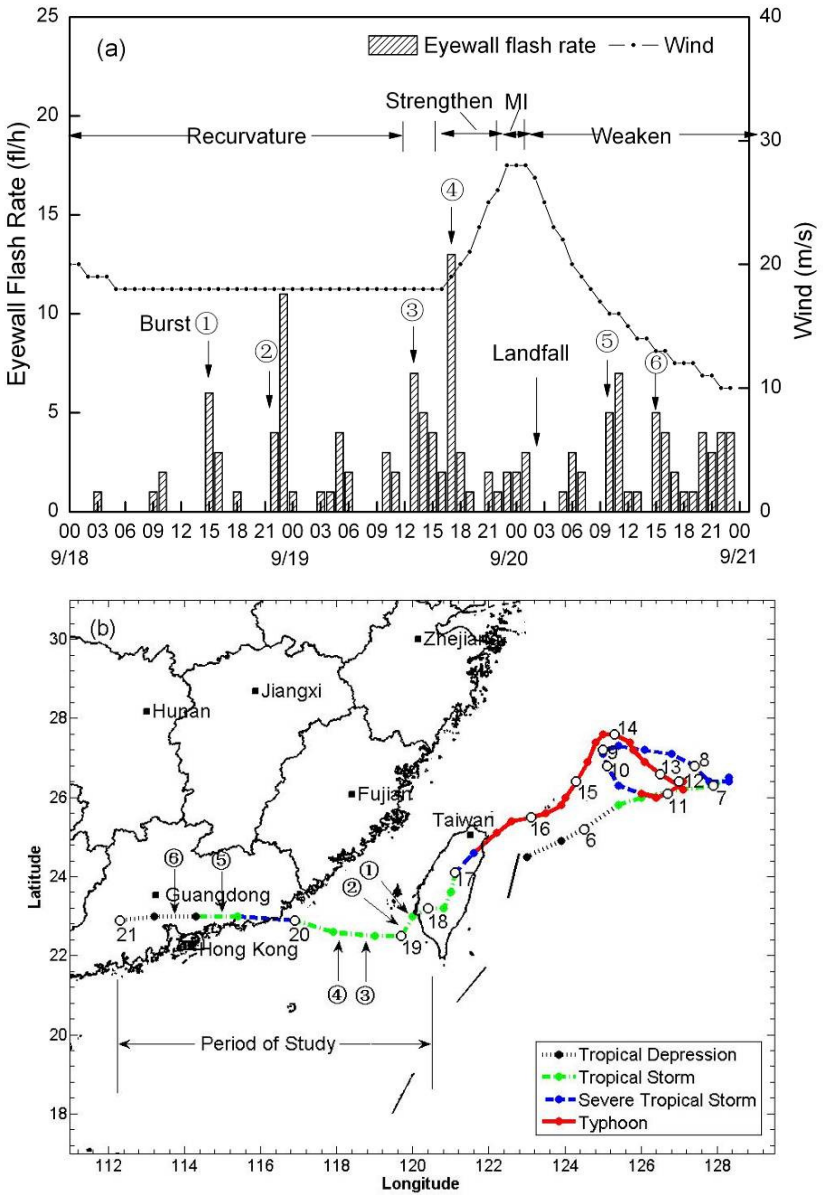

FIG. 5. Eyewall lightning outbreaks of Typhoon Nari (0116). (a) Temporal evolution of eyewall lightning, superimposed on hourly maximum sustained wind speed. (b) Best-track positions for the life cycle. The dotted line denotes tropical depression status, the dash-dot line tropical storm, the dashed line severe tropical storm, and the solid line typhoon. Open circles mark the 0000 UTC positions. The numbers next to the open circles indicate the dates in September 2001. Arrows with serial numbers in both figures indicate the six times of eyewall outbreaks. The period of study is between 0000 UTC 18 and 0000 UTC 21 September.

4. CONCLUSIONS

Cloud-to-ground lightning data from a regional lightning detetciton network in China have been used to analysis lightning activities in tropical cyclones at different intensity levels during the peirod of landfall, and to investigate the predictive value of eyewall flash outbreaks to changes of intensity and trajectory in storms.In the near future, we intend to combine our

results of eyewall lightning outbreaks with data from land-based radar and TRMM satellite, to obtain the internal precipitation structure for storms experienced eyewall outbreaks, and to investigate the relationship between eyewall lightning and convection morphology during the stages of storm weakening and recurvature.

5. ACKNOWLEDGEMENTS

This work was supported by the Basic Scientific Research and Operation Fund of Chinese Academy of Meteorological Sciences (2010Z004), the R&D Special Fund for Public Welfare Industry (GYHY201006005) and the Natural Science Foundation of China (41005006).

6. REFERENCES

Abarca, S. F., K. L. Corbosiero, and D. Vollaro, 2011: The World Wide Lightning Location Network and convective activity in tropical cyclones. *Mon. Wea. Rev.*, 139, 175–191.

China Meteorological Administration (CMA), 1999-2010: *Yearbook of Tropical Cyclone.* Beijing: China Meteorological Press (in Chinese).

Fierro, A. O., L. Leslie, E. Mansell, J. Strake, D. MacGormand, and C. Ziegler, 2007: A high resolution simulation of the microphysics and electrification in an idealized hurricane-like vortex. *Meteorol. Atmos. Phys.,* **98,** 13–33.

Fierro, A. O., X. M. Shao, T. Hamlin, J. M. Reisner, and J. Harlin, 2011: Evolution of eyewall convective events as indicated by intra-cloud and cloud-to-ground lightning activity during the rapid intensification of hurricanes Rita and Katrina. *Mon. Wea. Rev.,* **139,** 1492–1504.

Lyons, W. A., and C. S. Keen, 1994: Observations of lightning in convective supercells within tropical storms and hurricanes. *Mon. Wea. Rev.,* **122(8),** 1897–1916.

Molinari, J., P. K. Moore, and V. Idone, 1999: Convective structure of hurricanes as revealed by lightning locations. *Mon. Wea. Rev.,* **127,** 520–534.

Molinari, J., P. K. Moore, V. P. Idone, R. W. Henderson, and A. B. Saljoughy, 1994: Cloud-to-ground lightning in Hurricane Andrew. *J. Geophys. Res.,* **99,** 16665–16676.

Price, C., M. Asfur, and Y. Yair, 2009: Maximum hurricane intensity preceded by increase in lightning frequency. *Nature Geoscience,* **2:** 329–332.

Samsury, E., and R. E. Orville, 1994: Cloud-to-ground lightning in tropical cyclones: A study of Hurricanes Hugo (1989) and Jerry (1989). *Mon. Weather Rev.,* **122(8),** 1887–1896.

Squires, K., and S. Businger, 2008: The morphology of eyewall lightning outbreaks in two category 5 hurricanes. *Mon. Wea. Rev.,* **136:** 1706–1726.

Thomas, N. J., N. N. Solorzano, S. A. Cummer, and R. H. Holzworth, 2010: Polarity and energetics of inner core lightning in three intense North Atlantic hurricanes. *J. Geophys. Res.,* **115,** A00E15, doi:10.1029/2009JA014777.

Willoughby, H. E., 1990: Temporal changes of the primary circulation in tropical cyclones. *J. Atmos. Sci.,* **47,** 242–264.